

# Reducing CO2 footprint through synergies in carbon free energy vectors and low carbon fuels

Wang, W., Herreros, J. M., Tsolakis, A., York, A. P. E.

Author post-print (accepted) deposited by Coventry University's Repository

## Original citation & hyperlink:

Wang, W, Herreros, JM, Tsolakis, A & York, APE 2016, 'Reducing CO2 footprint through synergies in carbon free energy vectors and low carbon fuels' Energy, vol 112, pp. 976-983. DOI: 10.1016/j.energy.2016.07.010  
<https://dx.doi.org/10.1016/j.energy.2016.07.010>

DOI 10.1016/j.energy.2016.07.010

ISSN 0360-5442

ESSN 1873-6785

Publisher: Elsevier

***NOTICE: this is the author's version of a work that was accepted for publication in Energy. Changes resulting from the publishing process, such as peer review, editing, corrections, structural formatting, and other quality control mechanisms may not be reflected in this document. Changes may have been made to this work since it was submitted for publication. A definitive version was subsequently published in Energy VOL 112, (2016) DOI: 10.1016/j.energy.2016.07.010***

© 2016, Elsevier. Licensed under the Creative Commons Attribution-NonCommercial-NoDerivatives 4.0 International

<http://creativecommons.org/licenses/by-nc-nd/4.0/>

Copyright © and Moral Rights are retained by the author(s) and/ or other copyright owners. A copy can be downloaded for personal non-commercial research or study, without prior permission or charge. This item cannot be reproduced or quoted extensively from without first obtaining permission in writing from the copyright holder(s). The content must not be changed in any way or sold commercially in any format or medium without the formal permission of the copyright holders.

This document is the author's post-print version, incorporating any revisions agreed during the peer-review process. Some differences between the published version and this version may remain and you are advised to consult the published version if you wish to cite from it.

# Reducing CO<sub>2</sub> footprint through synergies in Carbon Free Energy Vectors and Low Carbon Fuels

W. Wang<sup>a</sup>, J.M. Herreros<sup>a</sup>, A. Tsolakis<sup>a\*</sup> and A.P.E. York<sup>b</sup>

<sup>a</sup>*School of Mechanical Engineering, University of Birmingham, Edgbaston, B15 2TT, UK*

<sup>b</sup>*Johnson Matthey Technology Centre, Blount's Court, Sonning Common, Reading RG4 9NH, UK*

\* Corresponding author. tel.: +44 (0) 121 414 4170, fax: +44 (0) 121 414 7484; a.tsolakis@bham.ac.uk

## Abstract

Carbon-footprint from transport and power generation can significantly be improved when carbon free or reduced carbon energy carriers are utilised that are compatible with the current technology of the internal combustion (IC) engines. The current study focuses on the reduction of diesel engine CO<sub>2</sub> emissions by improving ammonia and hydrogen combustion through the incorporation of alternative fuel, diethyl glycol diethyl ether (DGE) as an oxygenated fuel blend and combustion enhancer. The aim of the work is to study the potential synergies between DGE and two carbon free energy vectors H<sub>2</sub> and NH<sub>3</sub> in reducing the environmental effects and contribute in decarbonising internal combustion engines. DGE's ignition properties (i.e. high cetane number) improved the H<sub>2</sub> and NH<sub>3</sub> combustion efficiencies via counteracting their high auto-ignition resistances, and also contributing in lowering the unburnt H<sub>2</sub> and NH<sub>3</sub> emissions to the atmosphere. This led in the reduction of CO<sub>2</sub> by up 50% when 60-70% of diesel fuel is replaced with DGE, H<sub>2</sub> and NH<sub>3</sub>. Synergetic effects were also found between DGE and the gaseous fuels (i.e. hydrogen and ammonia) simultaneously decreasing the levels of PM, NO<sub>x</sub>, HC and CO emitted to the atmosphere; thus mitigating the health and environmental hazards associated to diesel engines.

**Keywords:** DGE, hydrogen, ammonia, pollutants, emission control

## 1. Introduction

Current worldwide transportation relies primarily on fossil fuels. Effective decarbonisation of the energy sector and especially transportation can be achieved by adopting fuel substitution with an energy carrier free of carbon. Ammonia (NH<sub>3</sub>) and hydrogen (H<sub>2</sub>) can be renewably resourced by utilising solar and wind energy. Hydrogen is believed to be one of the most potential alternatives [1] but due to its low volumetric energy density and infrastructure challenges associated with its transportation and handling, H<sub>2</sub> powered vehicles are still a niche product and widespread use is a

long term goal [2].

Ammonia has been studied as an energy [3] and hydrogen carrier for fuel cells [4, 5] and IC engines, providing that there is a process to split the  $\text{NH}_3$  into  $\text{N}_2$  and  $\text{H}_2$  [6]. In recent work we have proposed that this is feasible through the application of the catalytic ammonia reforming and decomposition using the heat of the engine exhaust gas to drive the reactions [2]. The combustion of reformed gas, i.e.  $\text{H}_2$ ,  $\text{N}_2$ ,  $\text{H}_2\text{O}$  and unconverted  $\text{NH}_3$ , in diesel engine with diesel fuels has shown to reduce carbonaceous emissions, including  $\text{CO}_2$ . However, under a range of engine operating conditions, higher  $\text{NO}_x$  emissions and incomplete combustion of the reformed gas was seen, similarly to LPG-diesel and natural gas-diesel dual fueled combustion, causing the production of other undesired emissions such as  $\text{NH}_3$  slippage [7]. Combustion improvements were observed in a study of LPG-diesel and CNG-diesel fueled diesel engine with the use of a high cetane number fuel, such as diethyl ether (DEE, CN >125) [8, 9]. Most recently, Ryu et al. [10] investigated the compression ignition combustion of ammonia and dimethyl ether (DME, CN = 60), where several appropriate strategies and fuel/gas mixtures were shown for the use of ammonia in direct-injection compression-ignition engines. Apart from that, DME is also referred as a cetane enhancer blended with different fuels/fuel mixtures for the purpose of particulate emission [11].

Similarly, diethyl glycol diethyl ether (DGE) can be regarded as another potential combustion enhancer based on its high cetane (CN = 140) number and its high content of fuel-born oxygen. Because of its featured high ignitability, DGE combustion in a diesel engine has a shorter ignition delay and was demonstrated to burn sufficiently in low-temperature combustion regime under charge-gas dilution and cooling [12]. All these characteristics of DGE can lead to the engine out improved  $\text{NO}_x$ /soot trade-off when it combusted with diesel fuel. Also as being similar to DEE, its presence (as fuel or fuel blend) in CI type of combustion is thought to be capable to assist the combustion of those less ignitable fuel alternatives, such as  $\text{H}_2$  and  $\text{NH}_3$ .

In this work the impact of  $\text{NH}_3$  and  $\text{H}_2$  combustion on the  $\text{CO}_2$  footprints of a diesel engine was studied. Following that, the addition of reduced carbon fuel, named DGE at different amounts into diesel, was studied as combustion improver of the carbon free gaseous fuels. The improvement in the properties of the diesel fuel (i.e. cetane number, ignition properties and presence of oxygen content) on the combustion and emission characteristics of the fuel mixture was assessed and compared in order to identify potential  $\text{CO}_2$  and other environmental benefits.

## 2. Experimental

*Test rig setup:* The  $\text{NH}_3$  reformat was simulated using  $\text{NH}_3$  and  $\text{H}_2$  gas bottles, whose flows were regulated by means of flow meters. The simulated gas additions were sent into the engine intake and premixed with the intake air. The liquid fuel (pure diesel or DGE blend) was injected into the cylinder to initiate the combustion. This approach required no modification to the fuel injection system. A Thring Titan thyristor-type DC electric dynamometer was used to motor and load the engine.

*Test engine:* The engine is a single-cylinder, direct injection, naturally aspirated diesel engine. The main engine specifications are: bore 98.4 mm, stroke 101.6 mm, conrod length 165.0 mm, displacement volume 773  $\text{cm}^3$ , compression ratio 15.5, maximum power 8.6 kW at 2500 rpm and maximum torque 39.2 Nm at 1800 rpm.

*Data acquisition:* The data acquisition and combustion analysis were carried out using in-house (University of Birmingham) developed Labview software. Output from the analysis of engine cycles included the in-cylinder pressure and rate of heat release (ROHR) at varying crank angle degrees, indicated mean effective pressure (IMEP), percentage coefficient of variation (COV) of IMEP values and other combustion characteristics.

*Emission analysis:* The gaseous emissions including  $\text{NO}$ ,  $\text{NO}_2$ ,  $\text{N}_2\text{O}$ ,  $\text{CO}$ ,  $\text{CO}_2$ , THC ( $\text{C}_1$  based) and  $\text{NH}_3$  were carried out by a MKS MultiGAS 2030 FTIR analyser (Fourier Transform Infrared Spectroscopy). Detection limits are 3.6 ppm for  $\text{NO}$ , 1.2 ppm for  $\text{CO}$  and lower than 1 ppm for the rest of gaseous species. Confidence intervals calculated using a 95% confidence level which reflects the reliability and repeatability of the equipment are shown in the results. FTIR results have been verified using known concentrations of  $\text{CO}_2$ ,  $\text{CO}$ ,  $\text{NO}$ ,  $\text{NH}_3$  and THC and a Horiba MEXA 7100DEGR ( $\text{CO}_2$  and  $\text{CO}$  by Non-Dispersive Infrared, oxygen ( $\text{O}_2$ ) by magnetopneumatic method,  $\text{NO}$  by Chemiluminescence Detection and HC by Flame Ionisation Detector) gas analyser was used to remove experimental bias during this procedure. Good agreement was obtained for the species and emission levels shown in this investigation. The hydrogen concentration in the exhaust was measured using a Hewlett Packard 5890 II gas chromatograph (GC) with thermal conductivity detector (TCD) using argon as carrier gas. An investigation of particulate matter (PM) was carried out using a TSI scanning mobility particle sizer (SMPS) 3080 electrostatic classifier to measure the particle size distribution. The sample was thermo-diluted using a rotating disk, with the dilution ratio set to 200:1

at 150 °C. Particulate measurement is focus on small particulates (in the range from 10 to 400 nm) being more dangerous for the environment and human health due to their higher reactivity, suspension time in the atmosphere and alveolar deposition fraction (especially ultrafine particulates lower than 100 nm).

*Liquid fuel:* Ultra-low sulphur diesel (ULSD) fuel was used as the primary liquid fuel for baseline operation. DGE was mixed volumetrically into the diesel to obtain the desired blends. Two blends with volumetric concentrations of 20 and 40% of DGE (DGE20 and DGE40 accordingly) were selected. This allowed a comparison between 3 different CN ratings and fuel-born oxygen contents. The fuel properties are listed in Table 1 for each tested fuel/fuel blend.

*Test combinations of gaseous additions:* In a previous on-board ammonia dissociation study using catalytic reforming technology [2], various amounts of hydrogen flow rates were produced under different reactor conditions. Unconverted  $\text{NH}_3$ ,  $\text{N}_2$  and  $\text{H}_2\text{O}$  (no  $\text{NO}_x$  production) make up the rest of the reactor product gas. For the purpose of current study, only  $\text{H}_2$  and  $\text{NH}_3$  were considered as the effective (combustible) reforming products; the obtained volumetric  $\text{H}_2$  to reformat ( $\text{H}_2 + \text{NH}_3$ ) ratio was ranging from 0.5 to 0.9, with roughly an increase of 0.1 from one reforming condition to another. Hence to simulate the reformat gas at higher flow rate, the observed  $\text{H}_2$ /reformat ratio was applied. The  $\text{H}_2$  flows were chosen at 10, 15 and 20 l/min with various amounts of  $\text{NH}_3$  selected accordingly to meet the actual  $\text{H}_2$ /reformat ratios. Pure forms of  $\text{H}_2$  and  $\text{NH}_3$  were also adopted for comparison purpose. All the  $\text{H}_2$ - $\text{NH}_3$  combinations are listed in Table 2.

*Test procedures:* The experimental runs were carried out in three separate sets for diesel and two DGE blends i.e. DGE20 and DGE40. All tests were performed under steady – state conditions at a controlled engine speed of 1500 rpm and a constant engine load of 5 bar IMEP throughout representing about 65% of full engine load at this engine speed. In all test sets, the liquid fuel blend was used to start and warm up the engine. Then different flows of  $\text{NH}_3$  and  $\text{H}_2$  or both combined were added into the air intake. The amount of liquid fuel injection was modified accordingly after the gaseous additions to keep the engine running at the same load. At least 20 minutes was allowed in each run for stabilising the engine before any of the readings being taken.

### **3. Results and discussion**

#### **Liquid fuel replacement**

The liquid fuel replacements on mass bases by the same quantity of gaseous fuels was higher in the case of diesel fuel when compared to DGE-diesel blends as shown in Figure 1. As the DGE content in the fuel blends was increased the amount of liquid fuel being replaced was reduced. This was due to the lower LHV (i.e. higher fuel-born oxygen content, Table 1) of DGE than that of diesel which increased the amount of DGE blend to keep the same engine load.

#### Combustion characteristics

The in-cylinder pressure and rate of heat release (ROHR) of diesel and diesel-DGE blends with different gaseous additions are plotted in Figure 2a and b. While the addition of  $\text{NH}_3$  (14 l/min) prolonged the ignition delay in diesel combustion (Figure 2a), the DGE's high ignitability (see Table 1) balances out the  $\text{NH}_3$ 's properties of high auto-ignition temperature ( $651^\circ\text{C}$ ) and octane rating (120) [10] as can be observed by the advanced start of the combustion. It is suggested that the  $\text{NH}_3$ /air pre-mixture being carried into the liquid fuel (diesel-DGE) spray periphery. When the liquid fuel ignited, a flame was propagated to initiate the combustion of the mixture (premixed DGE/diesel/ $\text{NH}_3$ /air) [9]. The beneficial effects of the oxygen content in DGE molecule could partially compensate the effects of the reduction in the overall air/fuel ratio due to the oxygen dilution (decrease in the intake air) from the incorporation of gaseous fuels at the air intake. By increasing the local oxygen/fuel ratio the oxidation of the gas/fuel mixture was also facilitated. In addition, the DGE's lower compressibility than diesel (usually inverse to density, see Table 1) could result in advanced fuel injection and ignition that in turn benefits also the  $\text{NH}_3$  ignition.

In the case of hydrogen addition, its high auto-ignition temperature and poor cetane rating did not retard the start of combustion and that was the case in presence or not of ammonia (Figure 2). This is due to the low ignition energy requirement for hydrogen (0.02 MJ/kg at stoichiometric  $\text{H}_2$ /air mixture) being even lower than for many of the hydrocarbon components of the fuels [13, 14].

In terms of the ROHR patterns, the combustion of the diesel- $\text{NH}_3$  mixture intensified the premixed phase and resulted in shorter combustion duration compared to diesel only combustion. This was suggested to be due to the combustion of  $\text{NH}_3$  and a high proportion of diesel in the premixed combustion (because of the longer available time to mix air,  $\text{NH}_3$  and the liquid diesel). On the other hand, can be suggested that hydrogen's higher flame speed [15, 16] when compared to diesel and  $\text{NH}_3$  led to faster and shorter combustion duration as can be seen by the larger increase in ROHR observed. The addition of DGE in diesel reduced the premixed combustion phase for the two DGE-diesel fuel

blends. This was due to the DGE's much higher cetane number (140) compared to that of diesel (53.9). As the DGE content increased, the ignition delay time was reduced and therefore suppressed the rate of heat release in premixed combustion.

Compared to the diesel baseline, the presence of the combined  $\text{NH}_3$  and  $\text{H}_2$  also intensified premixed combustion due to the rapid burning of  $\text{H}_2$  which thermally favoured the ignition and combustion velocity of  $\text{NH}_3$  [17] and/or even decompose  $\text{NH}_3$  into  $\text{H}_2$  and  $\text{N}_2$  [18]. These effects contributed to the largely increased peak ROHR and hence the in-cylinder temperature (reflected by the increased cylinder pressure) and shortened the overall combustion duration. The presence of DGE in the combined  $\text{NH}_3$ - $\text{H}_2$  combustion was again shown to reduce the intensity of the premixed combustion and increase the total combustion duration with respect to the diesel- $\text{NH}_3$ - $\text{H}_2$  combustion. The highest DGE concentration (i.e. DGE40) even further delayed the peak ROHR, which reduced therefore the peak cylinder pressure, indicating the decreased combustion temperature. The total combustion duration (combining the premixed and diffusion phases) and the ROHR in the diffusion phase increase for both of the gases when applied with the DGE blends. These were based on their diminished premixed phases, which indicate increased heat was released in the subsequent diffusion phase compared to the combustion with diesel. And the overall increased heat release duration of DGE than that of diesel in a broader range of in-cylinder conditions, enhances  $\text{NH}_3$  and  $\text{H}_2$  combustion.

The cyclic variation of the combustion was increased with  $\text{NH}_3$  and  $\text{H}_2$  addition, but the coefficient of variation (COV) of IMEP was kept under 7% for all the conditions. The engine instability could be derived from the increased incomplete combustion of these gaseous additions from one cycle to another. This point will be further proved in the following section, using the unburnt concentration of  $\text{H}_2$  and  $\text{NH}_3$ . The use of DGE improved the engine stability (COV of IMEP was lower than 3 for all the tested conditions) by its combustion characteristics described earlier i.e. a) reducing the cylinder pressure and hence the volatile in-cylinder condition through its low temperature combustion and b) improving the combustions of  $\text{H}_2$  and  $\text{NH}_3$  via its higher ignitability [19] and overall increased combustion duration.

#### $\text{CO}_2$ and unburned gaseous additions ( $\text{NH}_3$ and $\text{H}_2$ )

The trade-off between engine output  $\text{CO}_2$  emissions and the volumetric  $\text{NH}_3$  and  $\text{H}_2$  emissions under different fuelling conditions are shown in Figure 3a and b respectively. The ammonia measured

in the engine exhaust was reduced significantly by the addition of  $H_2$ . This was in accordance with the  $H_2$  improved  $NH_3$  combustion shown in Figure 2b. However, the unburned  $NH_3$  and  $H_2$  emissions are still high and other reasons such as  $NH_3$  and  $H_2$  escaping the combustion process during the process of charge exchange should be also considered.

*$NH_3$  and  $H_2$ :* As it is shown in Figure 3a and b, the presence of DGE also improved the emissions of  $NH_3$  and  $H_2$  for all the studied cases (diesel- $NH_3$ , diesel- $H_2$  and diesel- $H_2$ - $NH_3$  combustion). This is especially noticeable when higher additions of ammonia and hydrogen are used. DGE20 slightly improved unburnt  $NH_3$  emissions compared to diesel fuelling while the improvement was even further under the presence of hydrogen (Figure 3a). This is due to the beneficial effect of DGE20 on hydrogen combustion (Figure 3b) which also enhances  $NH_3$  combustion (synergetic effect) reducing the unburnt  $H_2$  and  $NH_3$  emissions. Further incorporation of DGE (DGE40) does not statistically significantly improve further hydrogen combustion, but reduces unburnt  $NH_3$  emissions.

The ignition properties of DGE enhanced the combustion pattern (see Figure 2), which improved also the ammonia and hydrogen combustion and hence reduced the unburnt ammonia and hydrogen due to, for example, the flame quenching on the chamber walls and the ammonia-air mixture trapped within the piston-ring crevice. The largest emissions of hydrogen and ammonia were recorded when DGE was absent and with a co-feeding of  $NH_3$  and  $H_2$  at 14 and 15 l/min. The combined gaseous addition replaced 29 l/min of the air intake flow, which represented 6% of air reduction in the overall intake charge. This brought the same dilution effect reducing the in-cylinder oxygen concentration (similarly to exhaust-gas-recirculation, EGR), which could result in incomplete combustion [20]. Furthermore the increased fuel replacement by high gaseous additions (Figure 1) also affects the diesel spray characteristics, which were thought to restrict the source of ignition for the gaseous additions. On the other hand, the low heating value of the DGE blends with respect to diesel results in a longer injection duration in addition to the longer combustion duration which increase the available time of the liquid fuel spray and diffusion combustion in the combustion chamber to ignite the gaseous fuels. Therefore, the fuel-born oxygen brought by DGE and DGE's high ignitability were inferred to alleviate the i) intake air shortage, ii) poor auto-ignition properties of the gaseous fuels and iii) reduction of the liquid fuel spray assisting the mixture's ignition and combustion.

*$CO_2$  emissions:* When  $NH_3$  is combusted the  $CO_2$  emissions released to the atmosphere are significantly reduced due to the absence of carbon in the  $NH_3$  molecule, but high unburnt  $NH_3$  was



released to the atmosphere resulting in a CO<sub>2</sub>-NH<sub>3</sub> trade off (Figure 3a). The incorporation of H<sub>2</sub> to diesel-NH<sub>3</sub> combustion enables to simultaneously decrease further the engine output CO<sub>2</sub> and NH<sub>3</sub> emissions. However, for high H<sub>2</sub> and NH<sub>3</sub> intake concentrations there is some unburnt hydrogen which is not efficiently combusted (Figure 3b). The use of DGE-diesel blend decreased the tank-to-wheel (TTW) CO<sub>2</sub> emissions due to the high O/C ratio compared to diesel combustion. The incorporation of DGE into the liquid diesel fuels enhances the combustion of the carbon free gaseous fuels (H<sub>2</sub> and NH<sub>3</sub>) and simultaneously decreases the engine output levels of CO<sub>2</sub>, NH<sub>3</sub> and H<sub>2</sub> released to the atmosphere. The reduction of CO<sub>2</sub> reached approximately 50% of the initial CO<sub>2</sub> emission recorded from the combustion of diesel fuel only.

From the results presented above, it is suggested the large decrease in engine output NH<sub>3</sub> emissions could be due to a number of phenomena, where the DGE could first enhance the individual combustions of H<sub>2</sub> and NH<sub>3</sub>, and more importantly, the improved H<sub>2</sub> combustion and its fast flame speed and propagation subsequently favouring the NH<sub>3</sub>'s combustion, resulting in a synergetic effect between the gaseous and liquid fuels overall improving the combustion process. This sequenced pattern is displayed in Figure 4.

#### Brake thermal efficiency

The brake thermal efficiencies (BTE) of the engine at different H<sub>2</sub>-NH<sub>3</sub> additions were calculated using Eq. 1 and are shown in Figure 5.

$$\eta = \frac{P_{\text{Brake}}}{(\text{LHV} \times M_f)} \quad \text{Eq. 1}$$

Where P<sub>Brake</sub> is the engine brake power, M<sub>f</sub> is the fuel mass flow rate and LHV is the lower heating value of each fuel and gas (i.e. Diesel, DGE, NH<sub>3</sub> and H<sub>2</sub>).

In general, the addition of H<sub>2</sub> and NH<sub>3</sub> into diesel operation decreased the engine thermal efficiency. This is associated with less efficient combustion of H<sub>2</sub> and NH<sub>3</sub> as described earlier with reference to Figure 3. Although the NH<sub>3</sub>'s combustion was enhanced by the presence of H<sub>2</sub>, it was not to the same extend as that of the baseline diesel. For a simple comparison, the hydrocarbon emission (C<sub>1</sub> based) at the 100% diesel baseline never exceeded 450 ppm at the studied load operation. In addition, part of the decrease could be also related to the intake air replacement by the H<sub>2</sub> and/or NH<sub>3</sub> that reduced the overall volumetric efficiency. Apart from the above, H<sub>2</sub> was reported to decrease the thermal efficiency in diesel combustion due to its higher flame velocity and small quenching distance

[21, 22] that increased heat loss to the chamber walls.

The DGE addition (DGE40, as an example) was shown to increase the BTE due to the improved  $H_2$  and  $NH_3$  utilisation as can be proved by the reduced emissions of  $H_2$  and  $NH_3$  under the DGE addition.

#### Other gaseous emissions

*CO and THCs:* Similar trends to  $CO_2$  are also observed for the emission reductions of CO and unburnt hydrocarbons (Figure 6a and 6b, respectively). The locally enriched fuel-born oxygen enhanced the complete fuel combustion, suppressing the formation of CO and THC [23]. In addition, the replacement of carbon based fuels, the more advanced ignition and overall prolonged combustion duration with the DGE blends (Figure 2b), increased the available time for CO and THC oxidation. The combustion properties of DGE are believed to support its easier (high CN rating) oxidation even in the late combustion stage, helping in removing the CO and THC that escaped from the main combustion events.

*$NO_x$  Emissions:* The PM- $NO_x$  emissions ( $NO + NO_2$ ) trade-off of the diesel and DGE blends with and without  $NH_3$  and  $H_2$  additions are plotted in Figure 7. Without hydrogen, the  $NO_x$  emission is shown to increase at small  $NH_3$  additions (up to 3 l/min). When larger quantities of ammonia were added, the effects of (i) low combustion flame temperature of  $NH_3$  [24] (ii) delayed start of combustion and consecutively retarded combustion, (iii) lower oxygen availability, all combined leading in suppressing  $NO_x$  production. As shown in the same plot, when the highest  $NH_3$  flow (14 l/min) was used, the  $NO_x$  emissions became even lower than that of the diesel baseline.

On the other hand, the improved  $NH_3$  combustion with hydrogen inevitably enhanced the NO and  $NO_2$  emission from that of the diesel baseline and is shown to be proportional to the hydrogen level (Figure 7). Although DGE was demonstrated to improve the  $NH_3$ 's combustion, further decrease in  $NO_x$  was observed due to the increased DGE presence (with and without the hydrogen addition). As indicated earlier in the combustion profile (Figure 2), the addition of DGE reduced the cylinder pressure (i.e. combustion temperature), especially in the premixed combustion phase where the  $NO_x$  formation is most significant. As a result,  $NO_x$  formation was further suppressed even the hydrogen promotion effect on  $NH_3$  combustion for the DGE40 blend.

On the other hand,  $N_2O$  emissions with the combined fuelling of  $H_2$ ,  $NH_3$  to liquid fuel combustion (for both diesel and DGE blends) were higher than those of just liquid fuel combustion. Around 10-15%

of the  $\text{N}_2\text{O}$  was reduced after the DGE blends being applied. This result needs to be further investigated in order to control  $\text{N}_2\text{O}$  emissions due to its high global warming potential.

#### Particulate matter emissions

The particulate size distribution and mass concentrations at different levels of DGE,  $\text{H}_2$  and  $\text{NH}_3$  are shown in Figure 8a-c and d-f respectively. The total PM emissions expressed in g/kWh are plotted in the  $\text{NO}_x$ -PM trade-off (Figure 7). The particle mass distribution was obtained from the particle number distribution through a size dependent agglomerate density function as described by Lapuerta et al. [25]. It has to be noted that only particulates in the range of 10 to 400 nm have been considered for the total PM estimation. In the case of larger particulates are included the PM emissions would be higher.

Combustion of the DGE blends showed simultaneous reductions in  $\text{NO}_x$  and PM emissions with and without gaseous additions, especially when 40% (v/v) of DGE is incorporated to the diesel fuel blend. The primary reason was again the oxygen present in the DGE molecule. This would allow enhanced combustion to take place even in the fuel rich area, which helped to oxidise the PM that were already formed or improve the oxidation of particles and particle precursors [26-28]. In addition to that, the prolonged combustion duration (Figure 2) at increased DGE level also provided longer time for the PM oxidation. Another reason for this PM reduction was based on the fact that DGE is in the form of ether [11, 29]. Due to its atomic structure of being one oxygen atom bound to two carbon atoms, the DGE structure was reported to effectively inhibit soot formation, which counts for a large portion in total PM.

After adding hydrogen and ammonia, the mass and number of PM were reduced for both diesel and DGE blends due to the large replacement of carbon through decreasing the formation of local fuel rich regions. The individual performance of  $\text{H}_2$  and  $\text{NH}_3$  are shown to improve at increased DGE level. This is supported by the reduced  $\text{H}_2$  and  $\text{NH}_3$  emissions shown earlier, meaning enhanced carbon replacement were achieved by better  $\text{H}_2$  and  $\text{NH}_3$  combustion. It is seen that  $\text{H}_2$  alone performed better in PM reduction than that of  $\text{NH}_3$ . This is in accordance with the more pronounced premixed phase in  $\text{H}_2$  combustion. The PM emission reduced when simultaneous additions of  $\text{NH}_3$  and  $\text{H}_2$  were adopted and decreased further with use of DGE. The number and mass particulate matter size distributions were decreased across the size spectrum (Figure 8), and hence decreased total mass emissions as shown in Figure 7. These trends further support the above proposed DGE combustion enhancement

(Figure 4), which in turn improved also the PM and NO<sub>x</sub> reduction.

#### **4. Conclusions**

Carbon free energy carriers and low carbon renewable fuels such as ammonia and hydrogen can be used in existing power generation technologies but there are challenges that need to be answered from the production to storage (especially on-board) and efficiency utilisation. In this research, the extent of the environmental benefits (i.e. CO<sub>2</sub> and other pollutants) that can be achieved when synergies in the utilisation of carbon free energy vectors (NH<sub>3</sub> and H<sub>2</sub>) and reduced carbon renewable fuels such as DGE are identified and assessed. These results are obtained for a research single cylinder engine. It is believed that quantitative results will depend on engine technology, but general trends and fundamental understanding of the roles of hydrogen and DGE on NH<sub>3</sub> combustion gained by this research are also applicable to modern multi-cylinder engines for practical applications. It has to be noted that the further potential to improve thermal efficiency and CO<sub>2</sub> emissions due to the possibility of using part of waste exhaust energy in the endothermic reforming process has not been considered. In addition, only the effects of the carbon-free fuels NH<sub>3</sub> and H<sub>2</sub> have been studied here, while the effects on combustion and emissions of N<sub>2</sub> produced by ammonia dissociation process have not been investigated as those effects have been already studied in the literature.

The study demonstrates that low carbon renewable fuels such as DGE, can directly impact in CO<sub>2</sub> emissions but most importantly can be designed to have the suitable properties to enhance the utilisation of carbon free energy carriers, in this case ammonia and hydrogen. By easing the utilisation of new environmentally friendly fuels and energy carriers, both CO<sub>2</sub> levels emitted to the atmosphere (up to 50% demonstrated here on tank-to-wheel bases) as well as other harmful pollutants can be depleted. The synergies between DGE and carbon-free gaseous fuels have also led in the reduction of other emissions (i.e. CO and hydrocarbons) and shifted the well-known diesel engine PM and NO<sub>x</sub> trade-off to lower values. In addition, the combination DGE's molecule oxygen content and good ignition properties allowed counteracting for the replacement of oxygen part of the air with the induction of gaseous fuel.

#### **Acknowledgments**

The authors would like to thank Johnson Matthey for funding the project. The School of Mechanical Engineering at the University of Birmingham (UK) is gratefully acknowledged for the

PhD School Scholarship to Mr. Wentao Wang. Engineering and Physical Science Research Council-EPSRC projects (EP/G038139/1) for supporting the research work. Advantage West Midlands and the European Regional Development Fund as part of the Science City Research Alliance Energy Efficiency Project are also acknowledged for supporting the research work.

## References

1. Tsolakis, A.; Megaritis, A., Catalytic exhaust gas fuel reforming for diesel engines—effects of water addition on hydrogen production and fuel conversion efficiency. *International Journal of Hydrogen Energy* **2004**, 29, (13), 1409-1419.
2. Wang, W.; Herreros, J. M.; Tsolakis, A.; York, A. P. E., Ammonia as hydrogen carrier for transportation; investigation of the ammonia exhaust gas fuel reforming. *International Journal of Hydrogen Energy* **2013**, 38, (23), 9907-9917.
3. Rees, N. V.; Compton, R. G., Carbon-free energy: a review of ammonia- and hydrazine-based electrochemical fuel cells. *Energy & Environmental Science* **2011**, 4, (4), 1255-1260.
4. Zhang, F.; Liu, J.; Yang, W.; Logan, B. E., A thermally regenerative ammonia-based battery for efficient harvesting of low-grade thermal energy as electrical power. *Energy & Environmental Science* **2015**, 8, (1), 343-349.
5. Rollinson, A. N.; Jones, J.; Dupont, V.; Twigg, M. V., Urea as a hydrogen carrier: a perspective on its potential for safe, sustainable and long-term energy supply. *Energy & Environmental Science* **2011**, 4, (4), 1216-1224.
6. Schuth, F.; Palkovits, R.; Schlogl, R.; Su, D. S., Ammonia as a possible element in an energy infrastructure: catalysts for ammonia decomposition. *Energy & Environmental Science* **2012**, 5, (4), 6278-6289.
7. Alam, M.; Goto, S.; Sugiyama, K.; Kajiwara, M.; Mori, M.; Konno, M.; Motohashi, M.; Oyama, K., Performance and Emissions of a DI Diesel Engine Operated with LPG and Ignition Improving Additives. *SAE International* **2001**, 2001-01-3680.
8. Miller Jothi, N. K.; Nagarajan, G.; Renganarayanan, S., LPG fueled diesel engine using diethyl ether with exhaust gas recirculation. *International Journal of Thermal Sciences* **2008**, 47, (4), 450-457.
9. Karabektas, M.; Ergen, G.; Hosoz, M., The effects of using diethylether as additive on the performance and emissions of a diesel engine fuelled with CNG. *Fuel* **2014**, 115, (0), 855-860.
10. Ryu, K.; Zacharakis-Jutz, G. E.; Kong, S.-C., Performance characteristics of compression-ignition engine using high concentration of ammonia mixed with dimethyl ether. *Applied Energy* **2014**, 113, (0), 488-499.
11. Smith, B. L.; Ott, L. S.; Bruno, T. J., Composition-Explicit Distillation Curves of Diesel Fuel with Glycol Ether and Glycol Ester Oxygenates: Fuel Analysis Metrology to Enable Decreased Particulate Emissions. *Environmental Science & Technology* **2008**, 42, (20), 7682-7689.
12. Ito, T.; Ueda, M.; Matsumoto, T.; Kitamura, T.; Senda, J.; Fujimoto, H., Effects of Ambient Gas Conditions on Ignition and Combustion Process of Oxygenated Fuel Sprays. *SAE International* **2003**, 2003-01-1790.
13. White, C. M.; Steeper, R. R.; Lutz, A. E., The hydrogen-fueled internal combustion engine: a technical review. *International Journal of Hydrogen Energy* **2006**, 31, (10), 1292-1305.
14. Heywood, J., *Internal Combustion Engine Fundamentals*. 2nd ed.; Mc Graw-Hill: New York, 1988.
15. Saravanan, N.; Nagarajan, G.; Sanjay, G.; Dhanasekaran, C.; Kalaiselvan, K. M., Combustion analysis on a DI diesel engine with hydrogen in dual fuel mode. *Fuel* **2008**, 87, (17–18), 3591-3599.
16. Liew, C.; Li, H.; Nuszowski, J.; Liu, S.; Gatts, T.; Atkinson, R.; Clark, N., An experimental investigation of the

combustion process of a heavy-duty diesel engine enriched with H<sub>2</sub>. *International Journal of Hydrogen Energy* **2010**, 35, (20), 11357-11365.

17. Joo, J. M.; Lee, S.; Kwon, O. C., Effects of ammonia substitution on combustion stability limits and NO<sub>x</sub> emissions of premixed hydrogen–air flames. *International Journal of Hydrogen Energy* **2012**, 37, (8), 6933-6941.

18. Li, J.; Huang, H.; Kobayashi, N.; He, Z.; Nagai, Y., Study on using hydrogen and ammonia as fuels: Combustion characteristics and NO<sub>x</sub> formation. *International Journal of Energy Research* **2014**, 38, (9), 1214-1223.

19. Goto, S.; Lee, D.; Wakao, Y.; Honma, H.; Mori, M.; Akasaka, Y.; Hashimoto, K.; Motohashi, M.; Konno, M., Development of an LPG DI Diesel Engine Using Cetane Number Enhancing Additives. *SAE International* **1999**, 1999-01-3602.

20. Tsolakis, A.; Megaritis, A.; Wyszynski, M. L.; Theinnoi, K., Engine performance and emissions of a diesel engine operating on diesel-RME (rapeseed methyl ester) blends with EGR (exhaust gas recirculation). *Energy* **2007**, 32, (11), 2072-2080.

21. Shudo, T., Improving thermal efficiency by reducing cooling losses in hydrogen combustion engines. *International Journal of Hydrogen Energy* **2007**, 32, (17), 4285-4293.

22. Shudo, T.; Nabetani, S.; Nakajima, Y., Analysis of the degree of constant volume and cooling loss in a spark ignition engine fuelled with hydrogen *International Journal of Engine Research* **2001**, 2, (1), 81-92.

23. Miyamoto, N.; Ogawa, H.; Nabi, M. N., Approaches to extremely low emissions and efficient diesel combustion with oxygenated fuels *International Journal of Engine Research* **2000**, 1, (1), 71-85.

24. Gross, C. W.; Kong, S.-C., Performance characteristics of a compression-ignition engine using direct-injection ammonia–DME mixtures. *Fuel* **2013**, 103, (0), 1069-1079.

25. Lapuerta, M.; Armas, O.; Gómez, A., Diesel Particle Size Distribution Estimation from Digital Image Analysis. *Aerosol Science and Technology* **2003**, 37, (4), 369-381.

26. Lapuerta, M.; Armas, O.; Herreros, J. M., Emissions from a diesel–bioethanol blend in an automotive diesel engine. *Fuel* **2008**, 87, (1), 25-31.

27. McCormick, R. L.; Ross, J. D.; Graboski, M. S., Effect of Several Oxygenates on Regulated Emissions from Heavy-Duty Diesel Engines. *Environmental Science & Technology* **1997**, 31, (4), 1144-1150.

28. Nord, K. E.; Haupt, D., Reducing the Emission of Particles from a Diesel Engine by Adding an Oxygenate to the Fuel. *Environmental Science & Technology* **2005**, 39, (16), 6260-6265.

29. Westbrook, C. K.; Pitz, W. J.; Curran, H. J., Chemical Kinetic Modeling Study of the Effects of Oxygenated Hydrocarbons on Soot Emissions from Diesel Engines†. *The Journal of Physical Chemistry A* **2006**, 110, (21), 6912-6922.

**Table captions**

**Table 1:** Fuel properties of the tested liquid fuel/blend.

**Table 2:** H<sub>2</sub> and NH<sub>3</sub> additions to the engine intake.

**Table 1**

	<b>ULSD</b>	<b>DGE</b>	<b>DGE20</b>	<b>DGE40</b>
<b>Chemical Formula</b>	$C_{14}H_{26.18}$	$C_8H_{18}O_3$	$C_{12.52}H_{24.16}O_{0.74}$	$C_{11.20}H_{22.36}O_{1.40}$
<b>Molar Mass (kg/kmol)</b>	194.18	162	186.24	179.16
<b>Density at 15 °C (kg/m<sup>3</sup>)*</b>	827.1	908	843.3	859.46
<b>LHV (MJ/kg)**</b>	42.99	31.4	40.49	38.10
<b>Cetane Number</b>	53.9	140	-	-
<b>C (wt%)</b>	86.52	59.2	80.67	75.02
<b>H (wt%)</b>	13.48	11.1	12.97	12.48
<b>O (wt%)</b>	0	29.7	6.36	12.50

\* Estimated based on volumetric fraction

\*\* Estimated based on mass fraction



**Table 2**

<b>H<sub>2</sub> (l/min)</b>	<b>20.0</b>				<b>15.0</b>				<b>10.0</b>				<b>0.0</b>			
<b>NH<sub>3</sub> (l/min)</b>	0.0	3.0	7.5	14.0	0.0	3.0	7.5	14.0	0.0	1.0	7.5	14	1.0	3.0	7.5	14.0
<b>H<sub>2</sub>/Reformate</b>	1.0	0.9	0.7	0.6	1.0	0.8	0.7	0.5	1.0	0.9	0.6	0.4	0	0	0	0

## Figure captions

**Figure 1:** Liquid fuel replacement by different  $H_2$  and  $NH_3$  additions.

**Figure 2:** In-cylinder pressure and ROHR of the combustions of diesel and DGE blends with (a) separate additions of  $NH_3$  and  $H_2$  and (b) simultaneous addition of  $NH_3$  and  $H_2$ , the flow rates for  $NH_3$  and  $H_2$  are 14 and 15 l/min respectively.

**Figure 3:**  $CO_2$  and unburned gaseous additions trade-off for (a)  $NH_3$  and (b)  $H_2$  at different fuelling conditions.

**Figure 4** Combustion pattern proposed for DGE enhanced  $NH_3$  and  $H_2$  combustion.

**Figure 5:** Engine brake thermal efficiencies of the combustions of standard diesel and DGE blend with different combinations of  $H_2$  and  $NH_3$ .

**Figure 6:** Carbonaceous gaseous emissions of diesel and DGE blends with different combined additions of  $H_2$  and  $NH_3$  (a) CO and (b) THC.

**Figure 7:**  $NO_x$ -PM trade off.

**Figure 8:** PM number distributions for PM (a) diesel, (b) DGE20 and (c) DGE40 and PM mass distributions for (d) diesel, (e) DGE20 and (f) DGE40

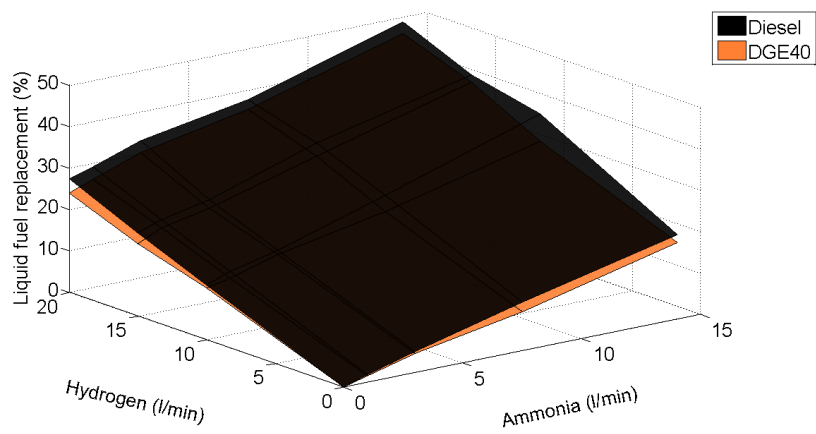


**Figure 1**

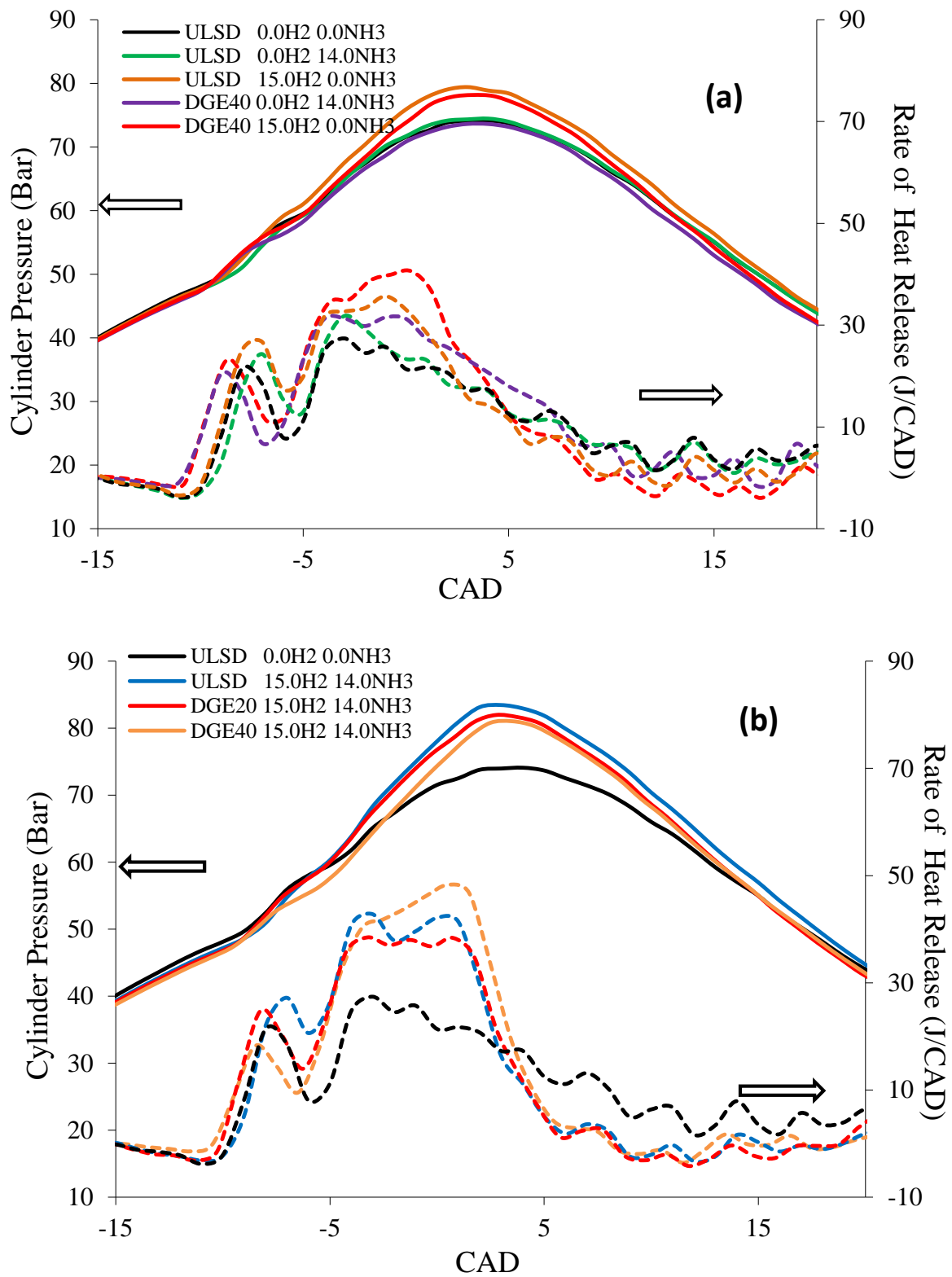


**Figure 2**

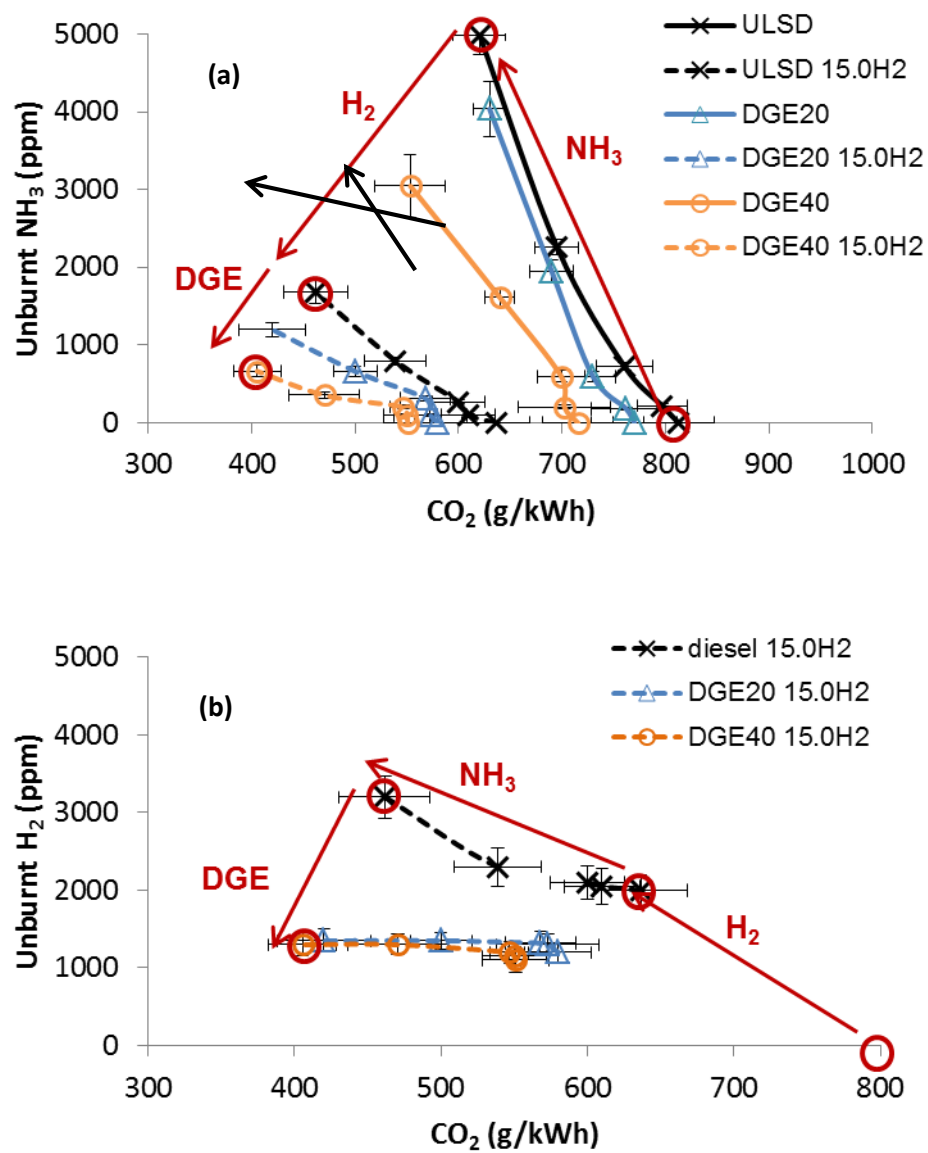
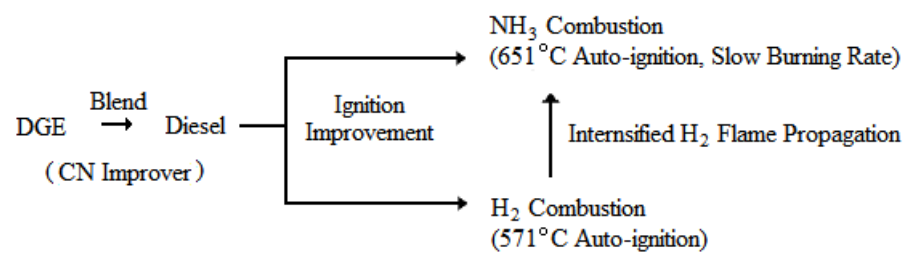
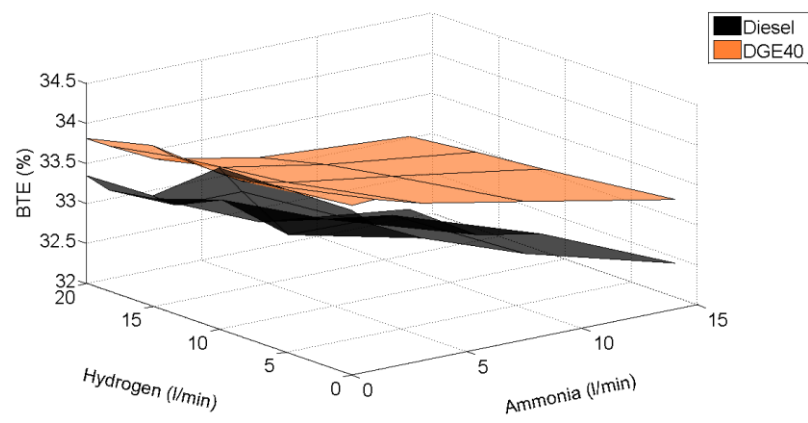


Figure 3



**Figure 4**



**Figure 5**

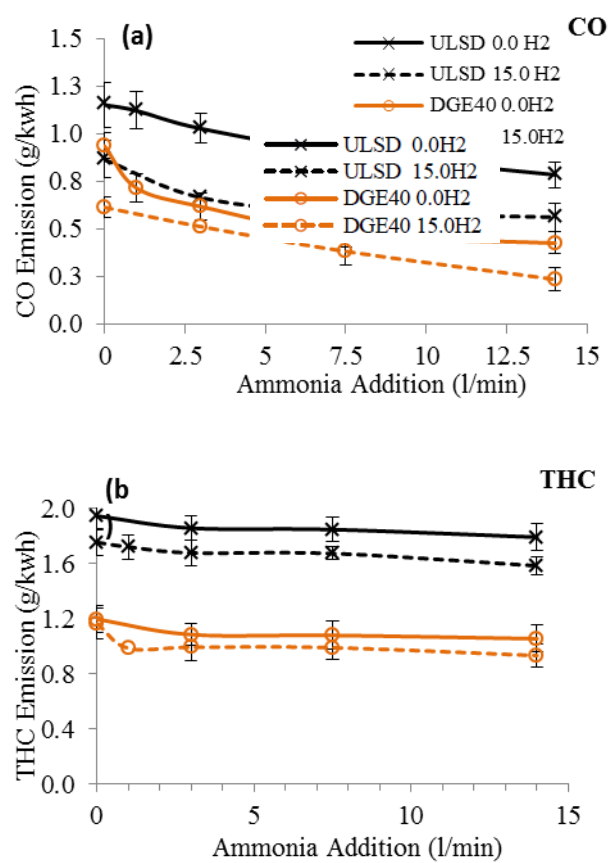


**Figure 6**



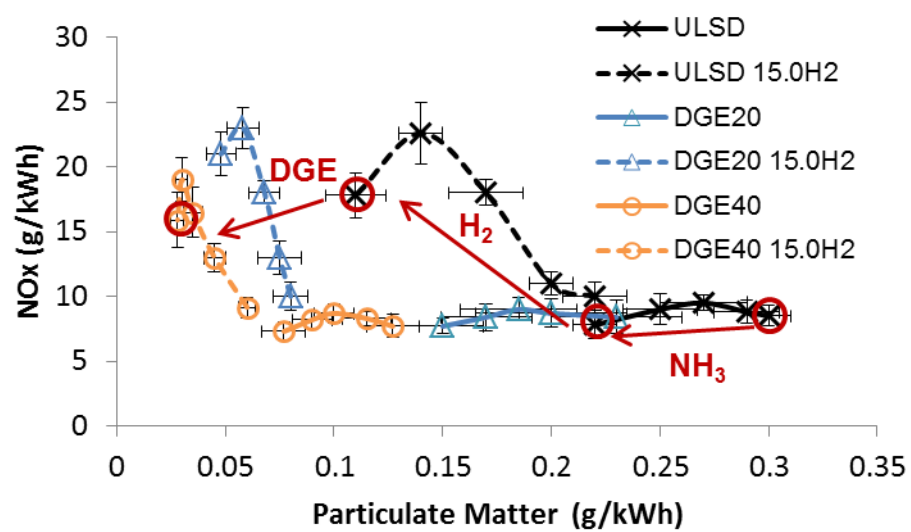
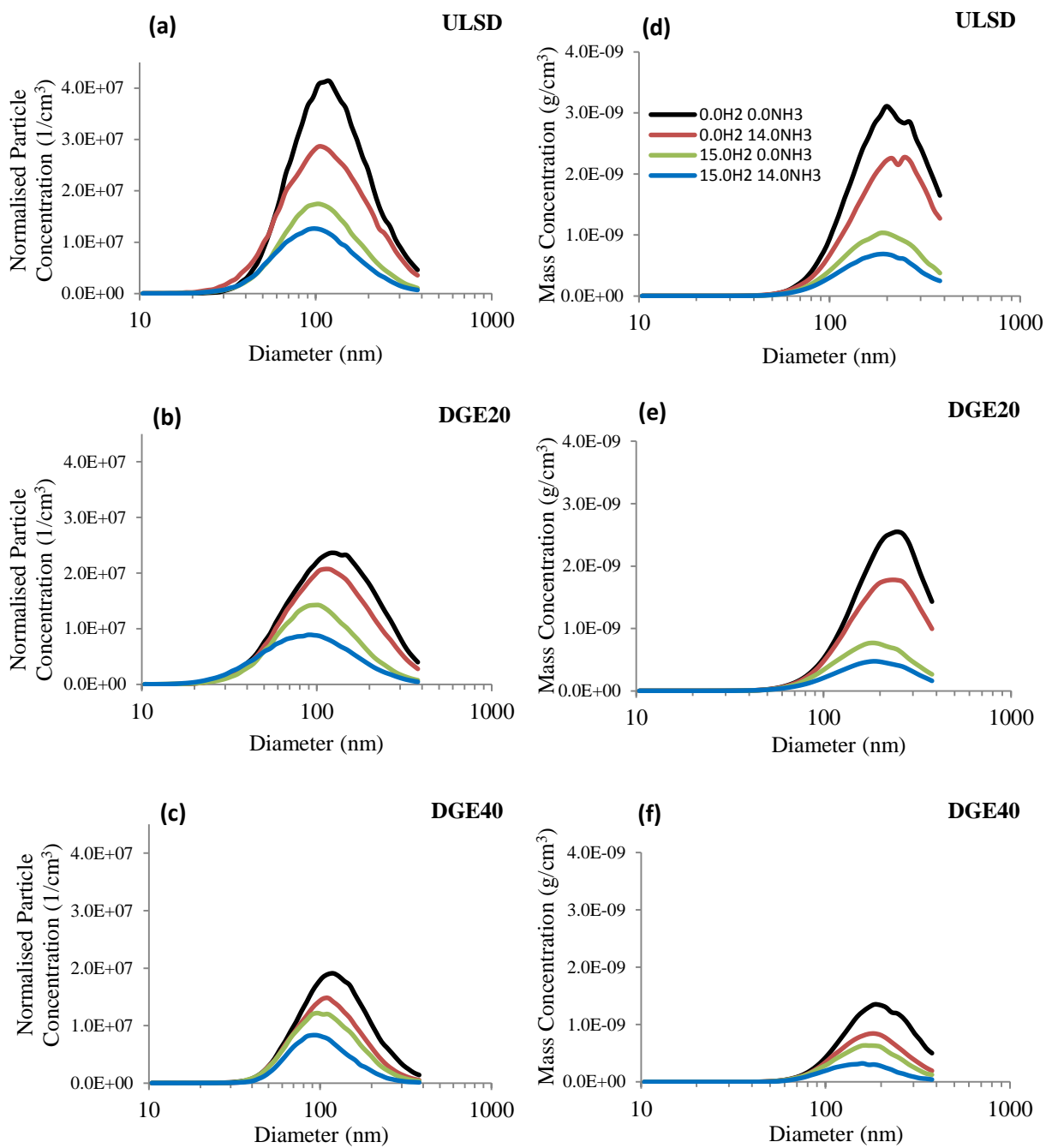


Figure 7



**Figure 8**